Macromolecules

ARTICLE

pubs.acs.org/Macromolecules

Influence of Solvent Polarity on the Self-Assembly of the Crystalline−Coil Diblock Copolymer Polyferrocenylsilane-*b*-polyisoprene

Fei Qi,[†,‡] Gerald Guerin,[†] Graeme Cambridge,[†] Wenguo Xu,[‡] Ian Manners,[§,*] and Mitchell A. Winnik[†,*]

[†]Department of Chemistry, University of Toronto, 80 Saint George Street, Toronto, Ontario, Canada, M5S 3H6

[‡]Institute for Chemical Physics, School of Science, Beijing Institute of Technology, Beijing, P. R. China, 100081

[§]School of Chemistry, Bristol University, Bristol, United Kingdom, BS8 1TS

ABSTRACT: Many poly(ferrocenyldimethylsilane) (PFS) block copolymers form fiber-like micelles with a semicrystalline core in selective solvents. Solvent effects on micelle formation are not well understood. This paper compares micelle formation for a sample of PFS_{50}−PI_{1000} (the subscripts refer to the number-average degrees of polymerization) in decane with that in *tert*-butyl acetate (*t*BA), a more polar solvent. When micelle formation is seeded, by adding block copolymer as a concentrated solution in tetrahydrofuran to solutions of micelle fragments, micelle growth was similar in both solvents. Micelles with a narrow length distribution were formed and the length increased in proportion to the amount of polymer added. In contrast, when micelles were prepared by heating a sample of the block copolymer in decane or *t*BA to 90 °C and allowing the solution to cool, pronounced differences were observed. In decane, micelles with a uniform width (10 nm) and a length on the order of 5 μm formed after 1 h, and grew to about 10 μm after 5 days. In *t*BA, aliquots taken from solution 1 h after cooling appeared to undergo microphase separation only upon solvent evaporation. Ribbon-like structures were observed after 1 and 5 days aging, but these evolved into fiber-like structures with a uniform 10 nm width and lengths greater than 30 μm after 25 days. These differences observed in the rate of micelle formation likely reflect differences in the nucleation stage of micelle formation. *t*BA is a better solvent for the PFS block than decane. As a consequence, it appears to take much longer for semicrystalline micelle nuclei to form in *t*BA. The seeded growth experiments demonstrate that once seed micelles are present, growth occurs similarly in both solvents.

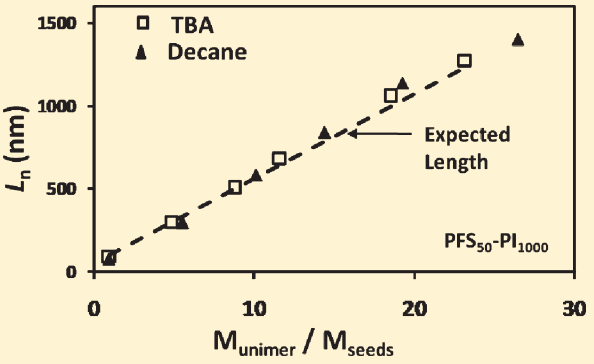

INTRODUCTION

Block copolymers self-assemble into micelles when they are dissolved in a selective solvent, a good solvent for one block and a poor solvent for the other block.[1] A variety of micelle morphologies can be obtained from the self-assembly of block copolymer. These include spheres, cylinders,[2] vesicles,[3] and more complex shapes.[4] Formation of cylindrical micelles are of special interest because these micelles have potential applications in flow-intensive drug delivery,[5] as additives for the enhancement of the toughness of epoxy resin[6] and as scaffolds or templates for the deposition of metal nanoparticles.[7] For micelles formed from block copolymers in which the insoluble block is not rigid or does not crystallize, the so-called "coil−coil" diblock copolymers, the most common micelles are spherical.[8] The formation of cylinders is limited to a narrow range of compositions with a nearly equal ratio of the two blocks.[9−12]

The term "crystalline−coil" block copolymers refers to diblock copolymers in which the insoluble block forms a semicrystalline phase. While the most common morphology for solution self-assembly of some crystalline−coil diblock copolymers are thin lamellae, some crystalline−coil block copolymer self-assemble into cylindrical micelles in selective solvents, and these fiber-like micelles form from block copolymer molecules with a wide range of block ratios. For example, poly(ferrocenyldimethylsilane-*b*-isoprene) (PFS−PI) is a crystalline−coil block copolymer that undergoes self-assembly in alkane solvents (e.g., decane or hexane), a solvent selective for the PI block.[13] Elongated micelles with semicrystalline cores are formed from PFS−PI polymers with compositions ranging from 15 wt %[14] to 78 wt % PFS.[12,15] Other examples of crystalline−coil block copolymers that have been shown to form cylindrical micelles include poly(acrylonitrile-*b*-methyl methacrylate) (PAN−PMMA), PAN−PS (PS = polystyrene),[16] and poly(caprolactone-*b*-ethylene oxide) (PCL−PEO).[17] Several studies suggest that crystallization is the driving force for the self-assembly of crystalline−coil block copolymer into cylindrical structures.[13,18]

A unique feature of PFS-based cylindrical micelles is that they exhibit "crystallization-driven living self-assembly". If one adds

Received: April 8, 2011
Revised: June 16, 2011
Published: July 14, 2011

more copolymer (dissolved in a common good solvent like tetrahydrofuran (THF)) to a solution of PFS block copolymer micelles in a selective solvent, the existing micelles grow longer. No new micelles are formed. If the added block copolymer has a different corona-forming block, then a new type of structure is formed, block comicelles.[15,19] This nucleated growth mechanism and bidirectional growth property of PFS block copolymer micelles are also interesting because the micelle growth process shows striking similarities with the formation of amyloid fibers.[20] PFS−PI micelles are also of special interest because of the redox or catalytic activity provided by the PFS block and the ability to form magnetic ceramic nanodomains.[21]

In this study, we focus on solvent effects on the self-assembly of a crystalline−coil block copolymer. Although the solvent interaction with polymer chains plays an important role in the formation of micelles, there are no systematic studies of solvent effects on micelles formed by crystalline−coil block copolymers. There are fewer publications about micelles formed by crystalline−coil block copolymers than by coil−coil block copolymers. In only a few of these studies were comments made about the influence of solvent quality or solvent polarity on the nature of the micelles formed. From our laboratory, Wang et al.[22] reported that the addition of THF to solutions of PFS−PI in decane slowed the rate of micelle formation and led to longer micelles. They suggested that this phenomenon might be related to the increased mobility of the PFS chains in the more polar solvent mixture. Lazzari et al.[23] examined the influence of solvent on the formation of fiber-like micelles by polyacrylonitrile-*block*-polystyrene (PAN-*b*-PS). They obtained longer micelles when they added chloroform (a selective solvent for PS) to a polymer solution in dimethylformamide (a common solvent for both blocks) than when they attempted direct dissolution of the polymer in chloroform itself. The authors also suggested that the common solvent enables easier growth in the length of the micelles.[23] Another study that invoked the influence of solvent on PFS block copolymer self-assembly was reported by Korczagin et al.[24] The authors examined the formation of cylindrical micelles by poly(ferrocenyldimethylsilane-*b*-methyl methacrylate) (PFDMS-*b*-PMMA) in acetone. They did not observe any crystalline peaks in wide-angle X-ray scattering data, and they argued based on NMR measurements that the PFS in the core of the micelle was not crystalline, and that "the contrast in polarity between the two blocks, supported by the polar block-selective solvent, rather than crystallization of the PFDMS block, is the primary driving force of PFDMS-*b*-PMMA micelle formation". From these results, it seems that both solvent polarity and the solubility of polymers in a particular solvent play a significant role in micelle formation for these block copolymers.

In this work, we describe the formation of micelles by PFS_{50}−PI_{1000} (the subscripts refer to the number-average degree of polymerization) in *tert*-butyl acetate (*t*BA), a relatively polar solvent that is still a good solvent for PI and a poor solvent for PFS. We followed the growth of these micelles by transmission electron microscopy (TEM) and dynamic light scattering (DLS) and compare micelle formation in *t*BA to micelle formation in decane.

EXPERIMENTAL SECTION

Materials. Decane (99+ %) and *tert*-butyl acetate (*t*BA) (99+ %) were purchased from Aldrich and used without further purification. The PFS_{50}−PI_{1000} (M_n = 81 400 g/mol, PDI = 1.02) block copolymer is the same sample described in ref 14.

Sample Preparation. *Direct Dissolution.* To obtain PFS_{50}−PI_{1000} micelle by direct dissolution, two sets of samples (0.2 mg/mL) were prepared, one in decane, and the other in *t*BA. Both solutions were prepared by adding a known quantity of polymer (0.4 mg) to ca. 2.0 mL of solvent. The solutions were heated in an oil bath at 90 °C for 30 min, and then allowed to cool to room temperature in air by removing the solutions from the heating bath. As these solutions aged at room temperature unstirred, aliquots, for TEM analysis, were taken at various time intervals to follow micelle growth. Micelle growth was deemed to be complete when the structures seen in successive TEM images did not change in length. Only very small amounts of sample were taken for these TEM measurements.

Seeded Growth. Seeded growth experiments began with the micelle solutions prepared as described above. After the growth of the micelles obtained by direct dissolution was deemed complete, the vials containing the solutions were reweighed to account for solvent evaporation, and the concentrations were recalculated. The remaining solution in each vial ($c \approx 0.2$ mg/mL) was sonicated to obtain shortened micelles. These micelle fragments were used as seeds for seeded growth experiments. Sonication experiments were carried out by immersing a sealed vial containing each sample into the water-containing chamber of a 70 W ultrasonic cleaning bath at ca. 23 to 25 °C. The *t*BA solution was sonicated for a total of 40 min, in four 10 min intervals. The decane solution was sonicated following a similar procedure, but only for two 10 min intervals. After sonication, the seed solutions in *t*BA or in decane were diluted to 0.02 mg/mL for the growth experiments.

The growth experiments were carried out by adding increasing amounts (4 μL, 21 μL, 38 μL, 50 μL, 80 μL, 100 μL) of PFS_{50}−PI_{1000} dissolved in tetrahydrofuran (THF, c = 9.3 mg/mL) to 2.0 mL aliquots of sonicated PFS_{50}−PI_{1000} micelles in *t*BA or in decane. As control experiments, a similar amount of THF (5 wt %) was added to an aliquot of the seed solution in *t*BA and to a similar seed solution in decane. After swirling to mix each of the growth solutions, they were allowed to age in the dark at room temperature. The growth was monitored by TEM until the length of the micelles did not change.

Transmission Electron Microscopy. Bright field TEM micrographs were obtained on a Hitachi H-7000 microscope operating at 100 kV. For TEM samples, a drop of micelle solution was placed on a carbon-coated copper grid. Excess fluid was then removed with a clean piece of filter paper. Images were analyzed using the software package Image J, published by the National Institutes of Health.[25] For the statistical length analysis, between 200 and 400 micelles were traced by hand to determine the contour length. The number-average micelle length (L_n) and weight-average micelle length (L_w) were calculated using eq 1, where N is the number of micelles examined in each sample, and L_i is the contour length of the i'th micelle.

$$L_n = \frac{\sum_{i=1}^{N} N_i L_i}{\sum_{i=1}^{N} N_i} \quad L_w = \frac{\sum_{i=1}^{N} N_i L_i^2}{\sum_{i=1}^{N} N_i L_i} \tag{1}$$

Wide-Angle X-ray Scattering. Samples for wide-angle X-ray scattering measurements were prepared by adding 2-propanol to a micelle solution (5 mg/mL) in *t*BA or in decane at room temperature. The micelles precipitated out of the solution and then were transferred onto an aluminum substrate followed by evaporation of the remaining solvent. WAXS diffraction data were obtained with an automated Siemens/Brukker D5000 diffractometer. The system is equipped with a high power line focus Cu Kα source operating at 50 kV/35 mA. The diffraction patterns were collected on a $\theta/2\theta$ Bragg−Brentano reflection geometry with fixed slits. A step scan mode was used for data acquisition with step size of 0.02° in 2θ and counting time of 1.5 s per step.

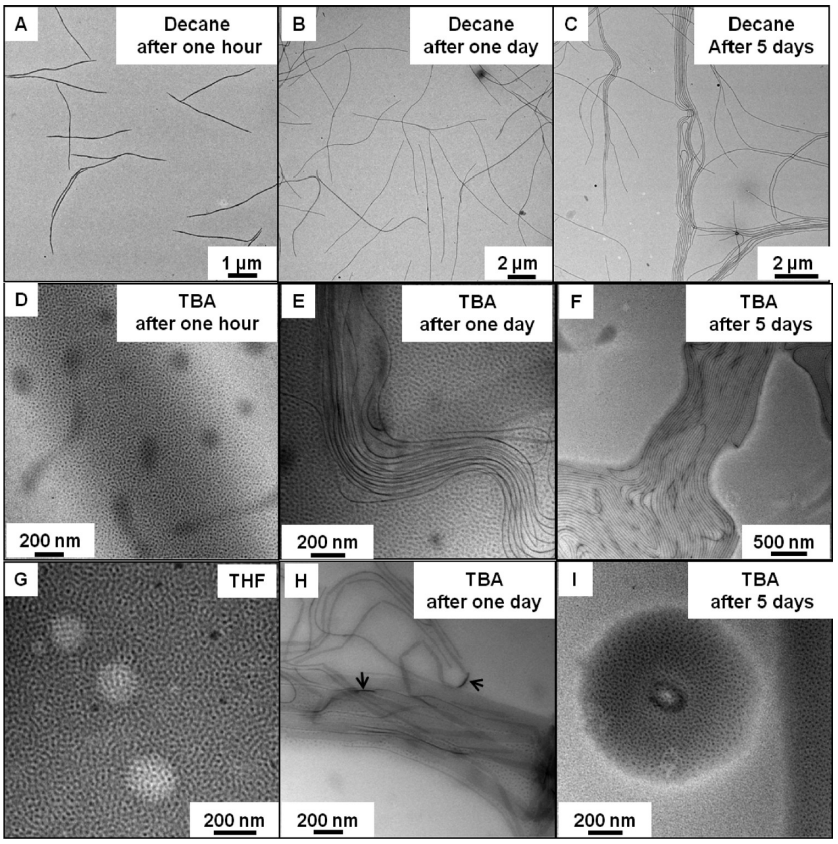

Figure 1. Comparison of TEM images of $PI_{1000}-PFS_{50}$ micelles formed ($c = 0.2$ mg/mL) in decane and in TBA at different aging times. $PI_{1000}-PFS_{50}$ micelles from decane, (A) 1 h after the solution was removed from the heating bath; (B) after 1 day and (C) after 5 days of aging at room temperature. Corresponding sample prepared in TBA, (D) after 1 h, (E) 1 day, and (F) 5 days. (G) TEM image of a grid prepared from a solution of $PI_{1000}-PFS_{50}$ in THF. (H) TEM image of a sample of another TBA solution prepared by the same protocol as that in part E. The arrows on this image point to darker parts of the micelles which we associate with twists. Part I presents a magnified image taken from the same grid as part F.

Light Scattering Experiments. For dynamic light scattering (DLS) experiments, each micelle solution was diluted to 0.01 mg/mL. Dynamic light scattering (DLS) measurements were performed using a wide angle light scattering photometer from ALV. The light source was a JDS Uniphase He−Ne laser ($\lambda_0 = 632.8$ nm, 35 mW) emitting vertically polarized light. The cells were placed into the ALV/DLS/SLS-5000 Compact Goniometer System and sat in a vat of toluene, which matched the index of refraction of the glass cells. The scattered light was detected by a Dual ALV-High Q.E. APD avalanche photodiode module, interfaced to the ALV-5000/EPP multiple-τ digital. All measurements were carried out at room temperature and at angle of 90°.

RESULTS

Micelles of $PFS_{50}-PI_{1000}$ were prepared both by direct dissolution and by seeded growth. In the sections below, we describe key features of the micelle formation and growth processes in decane and in *t*BA.

Direct Dissolution of PFS−PI Diblock Copolymer in Decane and in *t*BA. A sample of $PFS_{50}-PI_{1000}$ block copolymer was dissolved in decane (0.4 mg in 2.0 mL) by heating at 90 °C for 30 min. The solution became transparent and remained transparent after being cooled to room temperature and as the sample was aged. Aliquots were taken at different aging times for analysis by TEM. After the growth stopped, the solution was studied by DLS and by WAXS.

Selected TEM images of the micelle solution prepared in decane after different aging times are presented in Figure 1, parts A, B, and C. In bright-field TEM images, the electron-rich PFS domains appear dark. Figure 1A shows the TEM image of the sample prepared in decane 1 h after the solution was removed from the heating bath. Even at this short time, $PFS_{50}-PI_{1000}$ formed well-defined fiber-like micelles with a rather uniform width of ca. 10 nm. The mean length (L_n) calculated by analysis of this and other images was 5 μm. After 1 day of aging (Figure 1B), the micelles formed in the decane solution grew to 9.4 μm and maintained their uniform 10 nm width. After 5 days (Figure 1C), the mean length increased slightly ($L_n = 10\ \mu$m). After several more weeks, the mean length remained the same with no change in width. The constant length suggests that the micelles formed in decane had stopped growing within 5 days of aging.

Parallel experiments were prepared for a $PFS_{50}-PI_{1000}$ polymer sample at the same concentration in *tert*-butyl acetate. When the vial containing *t*BA and PFS−PI was heated, the block copolymer appeared by eye to dissolve more rapidly than the sample in decane, leading to a transparent solution. Interestingly, the solution remained clear after cooling to room temperature, but gradually turned cloudy as the solution was aged for several days. The suspension however remained colloidally stable for long aging times.

To compare the micelles formed in *t*BA and with those formed in decane, we also took aliquots for TEM analysis of the *t*BA

solution 1 h (Figure 1D) after removing the solution from the oil bath and allowing it to cool to room temperature, as well as after 1 day (Figure 1E) and 5 days (Figure 1F) of aging. Figure 1D shows a TEM image of $PFS_{50}-PI_{1000}$ micelles prepared in *t*BA 1 h after the solution was removed from the heating bath. Here we do not observe any long micelles. Instead we observe only grayish or dark ill-defined structures at low magnification. Higher magnification of one of these irregular structures is presented in Figure 1D. One can see within the gray areas well-defined patterns, including spherical domains, lamellae and hexagonal patterns. For comparison, we prepared a solution of $PFS_{50}-PI_{1000}$ in THF (a common good solvent for both blocks) at the same concentration as the solution in *t*BA (0.2 mg/mL). A TEM image (Figure 1G) prepared from this sample exhibits a similar pattern of lamellar and hexagonal structures. The similarities of the patterns in these images suggest that the structures observed in Figure 1D are due to microphase separation by unassociated block copolymers as the solvent evaporates. We will refer to the molecules that form these patterns upon drying as dissolved (or unassociated) chains.

After 1 day of aging (Figure 1E), we can see a bundle of long fibers surrounded by a thin film formed from dissolved chains. We also note in Figure 1E that the width of the fiber-like structures is not uniform, ranging from 10 nm (similar to the width of the micelles formed in decane) to 50 nm. The micelles with larger width appear lighter in color than the micelles that are 10 nm thick. To verify that we could reproducibly obtain structures with this variation in width, we prepared another sample in *t*BA using the same protocol. A TEM image from this solution after 1 day is presented in Figure 1H. Here we observe elongated micelles ranging from a width of 10 nm to more than 50 nm. Interestingly, in instances where these structures have a sharp turn, the micelles appear darker. The two arrows in Figure 1H point to these features. One interpretation of this type of image is that it is of a ribbon caught in a twist, with the enhanced contrast a result of the electrons passing edge-on through the structure. Figure 1F presents an image taken from a solution in *t*BA aged for 5 days. One can see long fiber-like structures that have a tendency to lie parallel to each other, accompanied by microphase separated domains resembling those seen at shorter times. A magnified image of one of these domains is shown in Figure 1I. The extended length of the fiber-like structures formed in *t*BA, and their tendency to aggregate, makes it difficult to measure their length.

After the *t*BA solution was aged for an additional 20 days at room temperature, no pools corresponding to $PFS_{50}-PI_{1000}$ free chains could be observed in TEM images. These results suggest that all of the polymer molecules at this time had been incorporate into micelles. Figure 2 shows TEM images of micelles formed in *t*BA after the growth stopped. We see very long micelles with discontinuous darker segments. A magnified image of two of these segments is presented in Figure 2B. These darker segments are small bundles of much shorter micelles of uniform 10 nm width that lie parallel to each other and appear to sandwich the longer micelles. Interestingly, the number of micelles in each bundle is always an odd number. One possible explanation for these structures is that the long micelles folded as they were deposited on the grid and sometimes broke into segments. Because the micelles themselves are so long, it is very difficult to measure their length. The micelle shown in Figure 2a, not counting the folds, is about 30 μm long. Figure 2C shows the TEM image of several micelles in another sample prepared in the same way in *t*BA. Again, the width appears to be uniform and 10 nm in diameter, and the micelles are longer than 30 μm.

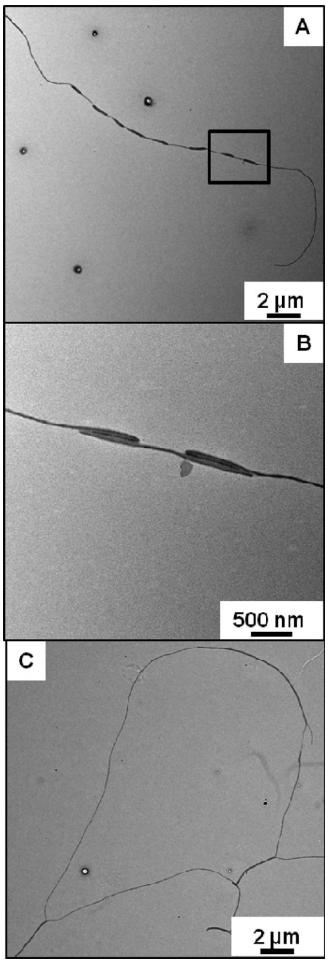

Figure 2. TEM images of $PI_{1000}-PFS_{50}$ micelles prepared in TBA after aging for 25 days at room temperature. (B) a magnified image of the structures (A) in the rectangular box. (C) A TEM image prepared from another sample in TBA after the same aging time.

We also examined these $PFS_{50}-PI_{1000}$ micelle solutions by dynamic light scattering (DLS) after the growth stopped. In Figure 3A, we present CONTIN plots for $PFS_{50}-PI_{1000}$ micelle solutions in *t*BA and in decane. For micelles formed in decane, we observe a large peak centered at a value of the apparent hydrodynamic radius R_h^{app} of ca. 400 nm with a weak second peak centered at $R_h^{app} = 60$ nm. This second peak might be due to the presence of shorter micelles, or it may be due to the effect of rotational modes or bending of the molecules for such elongated structures.[26] For micelles formed in *t*BA, we observe a large peak centered at a $R_h^{app} \approx 800$ nm, larger than the value for the sample in decane, and a second weak peak centered at $R_h^{app} = 80$ nm. The large peak for the *t*BA solution is significantly broader than the corresponding peak for the decane solution.

We investigated the crystallinity of the micelles after growth stopped by preparing films of micelle samples on aluminum foil substrates and examining them by WAXS. As shown in Figure 3B, we observe similar patterns for samples of micelles prepared in *t*BA and in decane. Both WAXS patterns show a broad peak corresponding to a *d*-spacing of 6.5 Å with a similar width at half height. Both show a large amorphous halo centered at ≈14° in

2θ. However, the peak from the decane sample is sharper and more intense relative to the amorphous halo than the peak from the *t*BA sample. The WAXS pattern from sample in *t*BA also shows a distinguishable, weak and broad peak at $2\theta = 15.1°$, which is not seen in the WAXS pattern of the decane sample.

Seeded Growth Experiments in Decane and in tBA. Previous experiments in our laboratory have shown that in decane, when PFS−PI micelles are sonicated, the micelles fracture to form shortened micelles (micelle fragments) without affecting the micelle width.[15] The termini of these shortened micelles remain active to the addition of PFS-based block copolymer in the form of an aliquot of polymer dissolved in a good solvent for both blocks.[19] This process is driven by epitaxial crystallization of the core-forming PFS block onto the ends of the micelle fragments, which act as seeds for further growth.

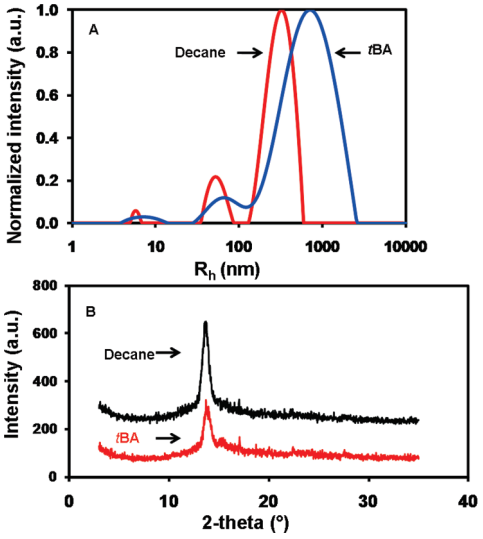

Figure 3. (A) CONTIN plots from DLS measurements on PFS_{50}−PI_{1000} micelles prepared in decane and in *t*BA. (B) WAXS patterns for PFS_{50}−PI_{1000} micelles prepared from micelle solutions in decane and in *t*BA. The weak sharp peak at $2\theta = 17°$ is from the aluminum substrate. The decane WAXS spectrum has been arbitrarily shifted up by 200 units for visual clarity.

To examine whether we could grow elongated micelles from fragments of micelles in *t*BA, we carried out experiments in parallel for samples of PFS_{50}−PI_{1000} micelles in *t*BA and in decane. Micelle solutions as described above were subjected to mild sonication to form fragments. The micelle solutions turned from turbid to clear during the sonication. A TEM image of the seed fragments obtained in *t*BA in this way is shown in Figure 4B. This can be compared to a very similar looking image of micelle fragments formed by sonication of micelles in decane shown in Figure 4A. In these images, the micelle width appears unchanged compared to the original long micelles. Corresponding histograms of the weight-average length distribution of seeds prepared in decane and in *t*BA are shown respectively in Figure 4, parts C and D. Analysis of the data for both solvents indicate a mean length of 50 nm (decane: $L_n = 50.9$, $L_w = 57.0$ nm; *t*BA: $L_n = 50.8$ nm, $L_w = 59.2$ nm).

For the growth experiment in *t*BA, we added small aliquots of a concentrated solution of PFS_{50}−PI_{1000} dissolved in tetrahydrofuran (THF) to solutions of the micelle fragments (seeds) in *t*BA. TEM images of each solution in *t*BA are shown in Figure 5. In these images, one can see well-defined elongated micelles with a uniform width of ca. 10 nm. The length of the micelles increased when more PFS_{50}−PI_{1000} in THF was added. Similar experiments were carried out in parallel for micelle fragments in decane. These results are shown as a series of TEM images in Figure 6. For all of the samples, values of L_w and L_n were obtained by TEM image analysis. In each instance, the ratio L_w/L_n was close to 1.1, indicating a narrow micelle length distribution.

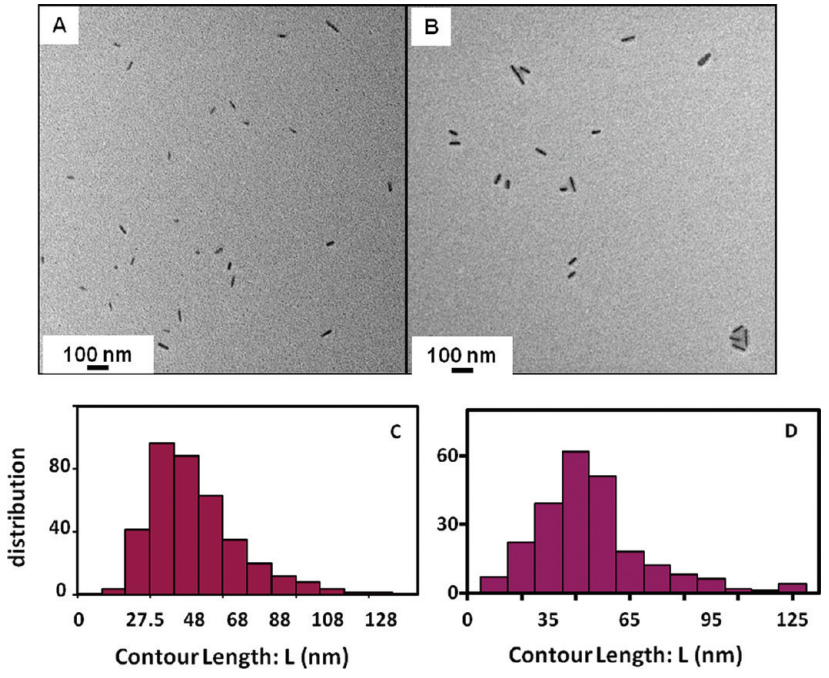

Figure 4. TEM images of sonicated PI_{1000}−PFS_{50} micelles prepared (A) in decane and (B) in TBA. (C and D) Histograms of the contour length distribution of the micelle fragments from (C) decane and (D) TBA.

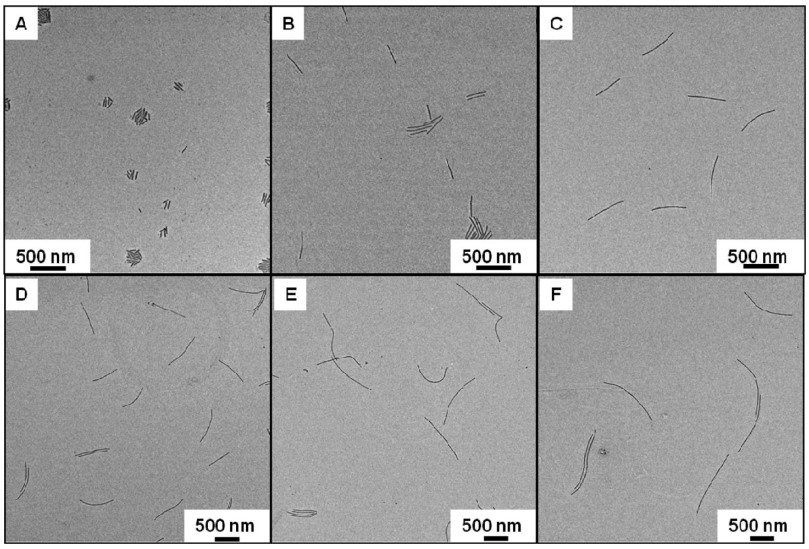

Figure 5. TEM images of $PI_{1000}-PFS_{50}$ micelles obtained by seeded growth experiments in *t*BA. Solutions of micelle fragments (2 mL, 0.02 mg/mL) were treated with (A) 4 μL, (B) 21 μL, (C) 38 μL, (D) 50 μL, (E) 80 μL, and (F) 100 μL of $PI_{1000}-PFS_{50}$ in THF (9.3 mg/mL). These solutions were then allowed to age for 1 week at 23 °C.

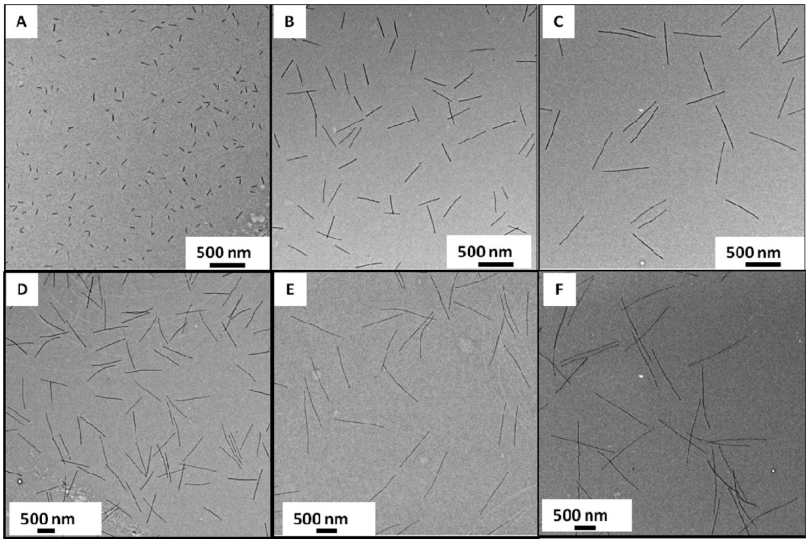

Figure 6. TEM images of $PI_{1000}-PFS_{50}$ micelles obtained by seeded growth experiments in decane. Solutions of micelle fragments (2 mL, 0.02 mg/mL) were treated with (A) 4 μL, (B) 23 μL, (C) 42 μL, (D) 60 μL, (E) 80 μL, and (F) 110 μL of $PI_{1000}-PFS_{50}$ in THF (9.6 mg/mL). These solutions were then allowed to age for 1 week at 23 °C.

This result is in agreement with the expectations for a seeded-growth process.

Values of L_n obtained by TEM analysis are plotted in Figure 7 against the ratio of the mass of added unimers over the mass of seed fragments in solution (M_{unimer}/M_{seeds}). The dashed line in Figure 7 is the predicted value for monodisperse rods as a function of polymer concentration assuming uniform growth of existing micelles.

DISCUSSION

The micelles formed by $PFS_{50}-PI_{1000}$ in decane and in *tert*-butyl acetate are very similar, in terms of the uniform 10 nm width seen in TEM images, in their X-ray diffraction patterns, and their elongation under seeded growth. These are all features of micelles with a semicrystalline PFS core, and the uniform width of the core suggests that the width is determined by the length and packing of the PFS chains in the core. The key feature in the WAXS spectra for micelles formed in both solvents is a prominent reflection at 6.5 Å. This peak, characteristic of PFS homopolymer samples crystallized from solution,[27] can be assigned to the distance between adjacent planes containing planar zigzag PFS chains.[28]

Some differences are apparent in the number of peaks that can be resolved in the WAXS spectra. When we compare the diffraction patterns obtained from *t*BA and decane, we notice a weak but discernible peak located at a *d* spacing of 5.87 Å. This weak peak is similar to a peak seen in X-ray patterns of oriented PFS homopolymer films reported by Papkov and co-workers.[29] They investigated X-ray diffraction patterns obtained from

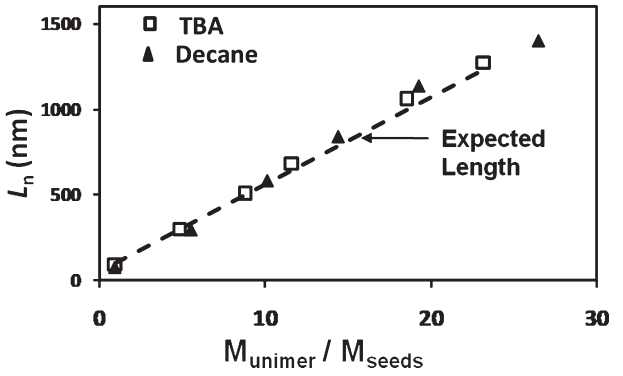

Figure 7. Plots of number-average contour length L_n of PI_{1000}−PFS_{50} micelles in TBA obtained from analysis of the TEM images in Figures 5 and 6 vs M_{unimer}/M_{seeds}. The dashed line is the prediction for uniform addition of polymer to the preformed seed fragments.

solution-cast nonoriented PFS films and films oriented by extrusion. They found that the intense 6.34 Å reflection in the as-cast films disappeared upon orientation and that the oriented films contained a more ordered crystalline structure. They assigned the four equatorial reflections at 6.63, 6.00, 5.60, and 5.32 Å in the oriented films to a monoclinic packing of PFS molecules in the (*ab*) crystallographic plane. The main conclusion of this part of their study was that the oriented films contained only one ordered (monoclinic) phase, which they referred to as phase I, whereas the unoriented samples contain an additional ordered phase (phase II). The limited number of reflections of this phase was more consistent with a partially ordered mesophase likely formed by conformationally disordered macromolecules. Since orientation leads to the disappearance of the 6.34 Å reflection but leaves the heat of fusion unchanged, they concluded that both phases coexist in the unoriented films. The WAXS spectra that we report in Figure 3 suggest the possibility that the proportions of the two phases in the micelle core may differ for micelles formed in the two solvents.

Seeded Growth. To carry out the seeded growth experiments, we took micelles prepared by direct dissolution and induced fragmentation by subjecting them to mild sonication using an ultrasonic cleaning bath. In our experimental design, we wanted to start with seed fragments of similar length (approximately 50 nm) for growth experiments in both solvents. We found that it took a longer time to achieve the desired micelle length in *t*BA (40 min) than in decane (20 min). This discrepancy in the sonication times is likely due to the higher vapor pressure of *t*BA (6.3 kPa), which decreases the sonication power compared with decane (0.17 kPa).[30] The micelle growth upon addition of free polymer dissolved in THF was remarkably similar in the two solvents as shown in Figure 7. Not only did micelle length increase in proportion to the amount of block copolymer added, the length followed the prediction of a model that assumed that all micelle fragments had two ends that were equally active to growth.

While we did not explicitly examine the rates of seeded micelle growth in the two solvents, they were not markedly different. Seeded micelle growth in *t*BA was substantially faster than the spontaneous micelle growth described in the following section.

Nucleation and Growth. Little is known about the influence of solvent on the formation of block copolymer micelles when the insoluble core is semicrystalline. This situation is very different than for coil−coil polymers, where solvent swelling of the core and solvent effects on the corona chain dimensions are known to affect micelle morphology. The self-assembly of coil−coil block copolymer is controlled primarily by interplay among the core−chain stretching, corona−chain repulsion and interfacial tension between the core and the solvent.[31] One can manipulate the morphology of these micelles by changing block copolymer-related properties, such as block ratio or nature of the blocks and solvent-related properties, such as polarity, presence of additives, copolymer concentration, the choice of solvent, or variation of the solvent/nonsolvent ratio.[1,32,33]

The classic examples come from the Eisenberg lab,[34] where he and his co-workers have obtained wide range of morphologies of polystyrene-*b*-acrylic acid (PS−PAA) block copolymer micelles, including spheres, rods, lamella and vesicles in aqueous solution, using polymers with different block ratios, or by adjusting the solution conditions.[35] These included variation of the common good solvent (DMF, dioxane, THF) and the amount of water as the nonsolvent used to induce self-assembly. Other interesting examples have been reported by Cheng et al.,[36] who studied the micelles formed by poly(styrene-*b*-ethylene oxide) (PS−PEO), and manipulated the micelle morphology by varying the selective solvent concentration.

For coil−crystalline block copolymers, there are some reports that polymer composition can affect the nature of the micelles formed. From our laboratories, Cao et al.[13] and Gädt et al.[15] found that PFS−PI samples with PFS block longer than or equal in length to the PI block formed lamellar micelles, whereas block copolymers in which the PI block was longer gave fiber-like micelles as seen here. Du et al.[37] observed a wider range of micelle morphologies with a change of block ratio of poly(ε-caprolactone)-*b*-poly(ethylene oxide) (PCL−PEO) under conditions where the PCL formed a semicrystalline core. In these polymers, the micelle morphology varied from spherical, rod-like, wormlike, to lamellar when the length of the PCL block was increased from 24 units to 142 units while PEO block was kept constant at ca. 44 units. In contrast, Lazzari and co-workers[38] found no effect of block ratio on the micelle morphology for polyacrylonitrile-based diblock copolymers. In their study, changing the block ratios in polyacrylonitrile/polystyrene (from 1:3 to 1:13) did not significantly affect the length of the cylindrical micelles.

As mentioned in the Introduction, there have been occasional descriptions of differences in micelle formation as a consequence of a change in solvent, but no systematic studies. An earlier report from our group mentioned that changing the micelle preparation conditions for PFS_{50}−PI_{250} using solvents such as hexane, decane or hexane/THF or hexane/toluene mixtures led to rod-like micelles similar in width but with lengths ranging from hundreds of nm to tens of micrometers.[22] This paper also reported that the presence of a small amount of THF in the hexane nonsolvent increased the micelle formation time of PFS−PI from 2 days to 1 week.

Here we find that upon direct dissolution and heating, micelle formation is much slower in *t*BA than in decane. There are many interesting differences in this process. For example, a newly formed solution of PFS_{50}−PI_{1000} in *t*BA, prepared by heating the mixture and cooling to room temperature, gave an image on a TEM grid (Figure 1D) that gave no indication of self-assembly in solution. Rather, the image was consistent with assembly of a block copolymer solution that underwent microphase separation as the solvent evaporated. A similar pattern was obtained from a solution of this block copolymer in THF, a common good solvent. There were other qualitative indications that *t*BA is a better solvent for PFS_{50}−PI_{1000} than decane. For example, the

Table 1. Solubility Parameters of Solvents Used [a]

	δ/MPa$^{1/2}$			
solvent	δ_t [b]	δ_d [b]	δ_p [b]	δ_H [b]
tetrahydrofuran	19.4	16.8	15.7	8.0
tert-butyl acetate	16.6	14.7	3.7	6.5
n-decane	15.8	15.8	0	0

[a] Data taken from ref 40. [b] δ_t total solubility parameter; δ_d dispersion parameter; δ_p polarity parameter; δ_H hydrogen bonding parameter.

solid dissolved rapidly upon gentle heating in *t*BA, whereas more forcing conditions were necessary in decane.

Differences in solubility are often explained in terms of solubility parameters. The value of the solubility parameter of PFS δ_{PFS} = 18.7 MPa$^{1/2}$,[39] while δ_{PI} = 17.0 MPa$^{1/2}$.[40] Table 1 lists the (overall) solubility parameters δ_t of the three solvents of interest to us (THF, *t*BA, decane), as well as a breakdown of the dispersion (δ_d), polar (δ_p), and hydrogen bonding (δ_H) components of the solubility parameters. From the more similar value of $\delta_{t,tBA}$ to δ_{PFS} than the corresponding value for decane, we would infer that PFS is more soluble in *t*BA than decane. One can also see in Table 1 that the magnitude of $\delta_{t,tBA}$ is influenced significantly by the polar contribution. While PFS itself appears to be a nonpolar polymer, local charge separation between the Fe atoms and the cyclopentadienyl rings plays an important role in determining the local conformation of the polymer in solution. We believe that these local dipoles lead to stronger interaction between PFS and *t*BA than between PFS and decane.[41]

Although solvent is known to have a strong influence on crystal growth and morphology,[42] we are unaware of studies of solvent effects on nucleation of polymer crystals. In contrast, there is a broader literature on solvent effects on protein crystallization. For example, Pan and co-workers[43] examined the protease subtilisin and observed that an increase in protein solubility induced by increasing the pressure led to a decrease in the crystal nucleation rate. In contrast, Gosavi and co-workers[44] reported for their system (chicken egg−white lysozyme) that increasing the solubility by adding acetonitrile led to an increase the nucleation rate of the protein crystals.

Another interesting difference in the formation of micelles by direct dissolution in decane and *t*BA is the formation of much longer micelles over the long time needed for these micelles to form. The most reasonable interpretation of this result is that nucleation is much slower in *t*BA than in decane. Not only is nucleation slower, but fewer nuclei form. The data in Figure 7 for seeded growth indicates that once nuclei are present, soluble polymer will deposit and grow epitaxially off the ends of these nuclei. For the direct dissolution experiments in decane, we find faster growth and shorter micelles. For *t*BA, even after 5 days (Figure 1, parts F and I), there is evidence for soluble polymer in the solution that forms microphase separation patters upon drying, in addition to long fiber-like micelles. There is no obvious indication of such patterns in images taken for micelles formed in decane, leading to the conclusion that nucleation of PFS crystallization is much faster in the poorer solvent. These findings can be compared to the results Monte Carlo simulations of single homopolymer chain crystallization by Wang.[45] This work indicates that in a good solvent, single polymer chains need an incubation period for nucleation, but not in a poor solvent.

There are some subtle features of self-assembly in *t*BA that we still do not understand. For the experiments described above, with a polymer concentration of 0.2 mg/mL, the evolution of PFS_{50}−PI_{1000} into long micelles occurred slowly and gradually. After only 1 day of aging in *t*BA, the polymer appeared to form ribbon-like structures. These ribbons disappeared over longer times, and after 5 days or more could no longer be detected. No short micelles were observed at any time in these experiments. Short micelles should be prominent at early stages of the aging process if micelle growth by deposition of polymer chains on nuclei was also slow. Another observation, that needs further investigation, is that at much higher polymer concentration in tBA (4 mg/mL) micelle growth was much faster (hours).

We have no evidence that phase separation in solution precedes or is involved in the nucleation process. We have some information about this possibility in a different system, PFS−P2VP (P2VP = poly(2-vinylpyridine)), which forms spherical amorphous micelles in methanol and long semicrystalline cylindrical micelles in 2-propanol.[46] In ethanol, the polymer initially forms amorphous spherical micelles. By TEM these spheres appear to aggregate, and on a time scale of months one sees the appearance of long cylindrical micelles.[47] There is no indication that the initially formed spherical micelles are the precursors of nuclei that form the semicrystalline long fiber-like structures. Similarly, we have no evidence that there is microphase separation in solution to form amorphous aggregates preceding the formation of the ribbon-like structures seen in Figure 1E for PFS_{50}−PI_{1000} in *t*BA after 1 day or the fiber-like micelles seen after 5 days in Figure 1F.

One should note that the micelle formation process that we described above is very different from that elucidated recently by Discher et al.[48] for the formation of worm-like micelles with a semicrystalline core by poly(ethylene oxide)-*b*-polycaprolactone (PEO−PCL) in water. Their experiments show that the fiber-like structure is determined by the composition of the block copolymer, and that the PCL core crystallizes after the fiber-like micelle is formed.

The final morphologies of PFS_{50}−PI_{1000} micelles formed in *t*BA and in decane are similar. In decane, we obtained well-defined fiber-like micelles with a width of ca. 10 nm and a length of ca. 10 μm. The micelles formed in *t*BA also have a width of ca. 10 nm, but were at least 3 times longer than micelles formed in decane. Because the starting concentration was the same for micelle solution in decane and in *t*BA, the fact that the micelles formed in *t*BA were so much longer suggests that fewer nuclei were formed. We need to explore whether the number of polymer molecules per unit length (the linear aggregation number) is similar in the micelles formed in these two solvents, as one might guess based on TEM dimensions. Light scattering experiments to determine these values are underway and will be reported in due course.

SUMMARY

This paper compares the formation of fiber-like micelles in decane with that in *tert*-butyl acetate (*t*BA) by a sample of PFS_{50}−PI_{1000}. When micelle formation is seeded, by adding polymer as a concentrated solution in tetrahydrofuran to solutions of 50 nm-long micelle fragments, micelle growth was similar in both solvents. Micelles with a narrow length distribution were formed and the length increased in proportion to the amount of polymer added to the seed solution. In contrast, when micelles were prepared by direct dissolution, i.e., heating a sample of the block copolymer in decane or *t*BA to 90 °C and

allowing the solution to cool, pronounced differences were found. In decane, micelles with a uniform width (10 nm) and a length on the order of 5 μm formed after 1 h, and grew to about 10 μm after 5 days. In *t*BA, aliquots taken from solution 1 h after cooling appeared to undergo microphase separation only upon solvent evaporation. Ribbon-like structures were observed after 1 and 5 days aging, but these evolved into fiber-like structures with a uniform 10 nm width and lengths greater than 30 μm after 25 days.

These differences observed in the rate of micelle formation likely reflect differences in the nucleation stage of micelle formation. We know from seeded growth experiments that when seed micelles as nuclei are present, growth occurs similarly in both solvents. *t*BA is a better solvent for the PFS component than decane. As a consequence, it appears to take much longer for semicrystalline micelle nuclei to form in *t*BA than in decane. We conclude that the rate at which micelles are formed spontaneously by $PFS_{50}-PI_{1000}$ in *t*BA and in decane is controlled by the rate of micelle nucleation.

AUTHOR INFORMATION

Corresponding Author

*E-mail: mwinnik@chem.utoronto.ca; ian.manners@bristol.ac.uk.

ACKNOWLEDGMENT

The authors thank NSERC Canada for their support of this research. I.M. thanks the European Union for a Marie Curie Chair and an Advanced Investigator Grant and the Royal Society for a Wolfson Research Merit Award.

REFERENCES

(1) Riess, G. *Prog. Polym. Sci.* **2003**, *28*, 1107–1170.
(2) Won, Y.-Y.; Davis, H. T.; Bates, F. S. *Science* **1999**, *283*, 960–963.
(3) Discher, B. M.; Won, Y.-Y.; Ege, D. S.; Lee, J. C.-M.; Bates, F. S.; Discher, D. E.; Hammer, D. A. *Science* **1999**, *284*, 1143–1146.
(4) Stewart, S.; Liu, G. *Angew. Chem., Int. Ed.* **2000**, *39*, 340–344.
(5) Geng, Y.; Dalhaimer, P.; Cai, S.; Tsai, R.; Tewari, M.; Minko, T.; Discher, D. E. *Nat. Nano.* **2007**, *2*, 249–255.
(6) Thio, Y. S.; Wu, J.; Bates, F. S. *Macromolecules* **2006**, *39*, 7187–7189.
(7) Cao, L.; Massey, J. A.; Winnik, M. A.; Manners, I.; Riethmüller, S.; Banhart, F.; Spatz, J. P.; Möller, M. *Adv. Funct. Mater.* **2003**, *13*, 271–276.
(8) Hamley, I. W. *Block Copolymers in Solution*; John Wiley and Sons Ltd: Chichester, West Sussex, England, 2005.
(9) Jain, S.; Bates, F. S. *Macromolecules* **2004**, *37*, 1511–1523.
(10) Zhulina, E. B.; Adam, M.; LaRue, I.; Sheiko, S. S.; Rubinstein, M. *Macromolecules* **2005**, *38*, 5330–5351.
(11) Choucair, A.; Eisenberg, A. *J. Am. Chem. Soc.* **2003**, *125*, 11993–12000.
(12) Qian, J.; Zhang, M.; Manners, I.; Winnik, M. A. *Trends Biotechnol.* **2010**, *28*, 84–92.
(13) Cao, L.; Manners, I.; Winnik, M. A. *Macromolecules* **2002**, *35*, 8258–8260.
(14) Cambridge, G.; Guerin, G.; Manners, I.; Winnik, M. A. *Macromol. Rapid Commun.* **2010**, *31*, 934–938.
(15) Gädt, T.; Ieong, N. S.; Cambridge, G.; Winnik, M. A.; Manners, I. *Nat. Mater.* **2009**, *8*, 144–150.
(16) Lazzari, M.; Scalarone, D.; Vazquez-Vazquez, C.; López-Quintela, M. A. *Macromol. Rapid Commun.* **2008**, *29*, 352–357.
(17) Geng, Y.; Discher, D. E. *J. Am. Chem. Soc.* **2005**, *127*, 12780–12781.
(18) Raez, J.; Manners, I.; Winnik, M. A. *J. Am. Chem. Soc.* **2002**, *124*, 10381–10395.
(19) Wang, X.; Guerin, G.; Wang, H.; Wang, Y.; Manners, I.; Winnik, M. A. *Science* **2007**, *317*, 644–647.
(20) Guérin, G.; Wang, H.; Manners, I.; Winnik, M. A. *J. Am. Chem. Soc.* **2008**, *130*, 14763–14771.
(21) Wang, X.-S.; Arsenault, A.; Ozin, G. A.; Winnik, M. A.; Manners, I. *J. Am. Chem. Soc.* **2003**, *125*, 12686–12687.
(22) Wang, X.; Liu, K.; Arsenault, A. C.; Rider, D. A.; Ozin, G. A.; Winnik, M. A.; Manners, I. *J. Am. Chem. Soc.* **2007**, *129*, 5630–5639.
(23) Lazzari, M.; López-Quintela, M. A. *Macromol. Rapid Commun.* **2009**, *30*, 1785–1791.
(24) Korczagin, I.; Hempenius, M. A.; Fokkink, R. G.; Cohen Stuart, M. A.; Al-Hussein, M.; Bomans, P. H. H.; Frederik, P. M.; Vancso, G. J. *Macromolecules* **2006**, *39*, 2306–2315.
(25) Collins, T. J. *BioTechniques* **2007**, *43*, S25–S30.
(26) Tracy, M. A.; Pecora, R. *Annu. Rev. Phys. Chem.* **1992**, *43*, 525–557.
(27) Lammertink, R. G. H.; Hempenius, M. A.; Manners, I.; Vancso, G. J. *Macromolecules* **1998**, *31*, 795–800.
(28) Rulkens, R.; Lough, A. J.; Manners, I.; Lovelace, S. R.; Grant, C.; Geiger, W. E. *J. Am. Chem. Soc.* **1996**, *118*, 12683–12695.
(29) Papkov, V. S.; Gerasimov, M. V.; Dubovik, I. I.; Sharma, S.; Dementiev, V. V.; Pannell, K. H. *Macromolecules* **2000**, *33*, 7107–7115.
(30) Muthukumaran, S.; Kentish, S. E.; Stevens, G. W.; Ashokkumar, M. *Rev. Chem. Eng.* **2006**, *22*, 155–194.
(31) Zhulina, Y. B.; Birshtein, T. M. *Polym. Sci. U.S.S.R.* **1986**, *28*, 2880–2886.
(32) Jain, S.; Bates, F. S. *Science* **2003**, *300*, 460–464.
(33) Li, Z.; Hillmyer, M. A.; Lodge, T. P. *Langmuir* **2006**, *22*, 9409–9417.
(34) Zhang, L.; Eisenberg, A. *Science* **1995**, *268*, 1728–1731.
(35) Shen, H.; Eisenberg, A. *J. Phys. Chem. B* **1999**, *103*, 9473–9487.
(36) Bhargava, P.; Zheng, J. X.; Li, P.; Quirk, R. P.; Harris, F. W.; Cheng, S. Z. D. *Macromolecules* **2006**, *39*, 4880–4888.
(37) Du, Z.-X.; Xu, J.-T.; Fan, Z.-Q. *Macromolecules* **2007**, *40*, 7633–7637.
(38) Lazzari, M.; Scalarone, D.; Hoppe, C. E.; Vazquez-Vazquez, C.; Lòpez-Quintela, M. A. *Chem. Mater.* **2007**, *19*, 5818–5820.
(39) Kulbaba, K.; MacLachlan, M. J.; Evans, C. E. B.; Manners, I. *Macromol. Chem. Phys.* **2001**, *202*, 1768–1775.
(40) Brandrup, J.; Immergut, E. H.; Grulke, E. A.; Abe, A.; Bloch, D. R. *Polymer Handbook*, 4th ed.; John Wiley & Sons, Inc: New York, 2005.
(41) Barlow, S.; Rohl, A. L.; Shi, S.; Freeman, C. M.; O'Hare, D. *J. Am. Chem. Soc.* **1996**, *118*, 7578–7592.
(42) Lahav, M.; Leiserowitz, L. *Chem. Eng. Sci.* **2001**, *56*, 2245–2253.
(43) Pan, X.; Glatz, C. E. *Cryst. Growth Des.* **2002**, *2*, 45–50.
(44) Gosavi, R. A.; Bhamidi, V.; Varanasi, S.; Schall, C. A. *Langmuir* **2009**, *25*, 4579–4587.
(45) Wang, M. *Phys. Lett. A* **2009**, *373*, 3285–3288.
(46) Wang, H.; Winnik, M. A.; Manners, I. *Macromolecules* **2007**, *40*, 3784–3789.
(47) Shen, L.; Wang, H.; Guerin, G.; Wu, C.; Manners, I.; Winnik, M. A. *Macromolecules* **2008**, *41*, 4380–4389.
(48) Rajagopal, K.; Mahmud, A.; Christian, D. A.; Pajerowski, J. D.; Brown, A. E. X.; Loverde, S. M.; Discher, D. E. *Macromolecules* **2010**, *43*, 9736–9746.